国立天文台
NAOJ
National Astronomical Observatory of Japan

光球・彩層の空間パワースペクトル フラックスチューブ成分はあるか

勝川行雄 (国立天文台)
D. Orozco Suarez (IAC)

Power spectrum of the surface convection

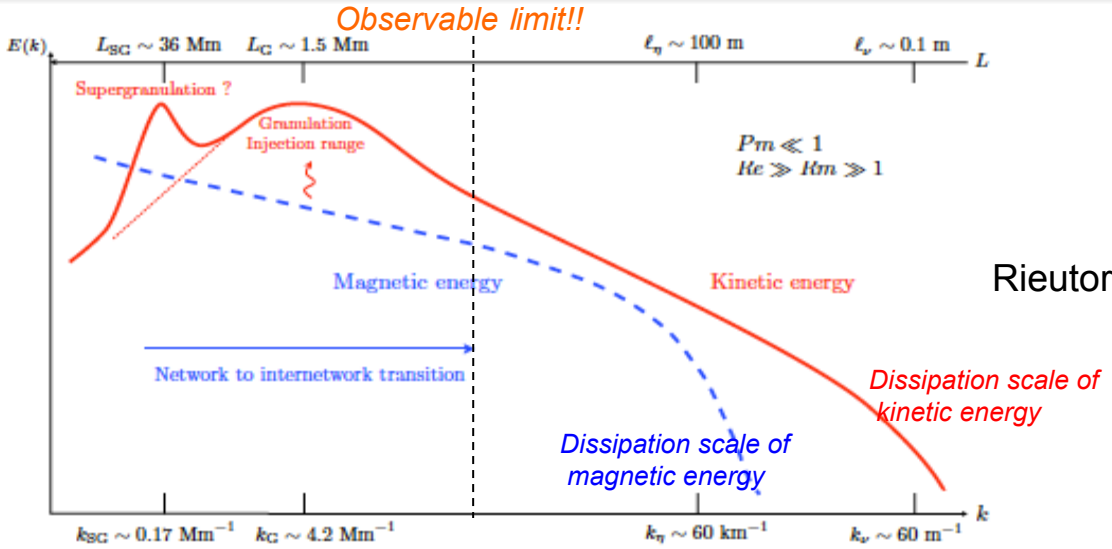

Rieutord and Rincon (2010)

- The power spectrum analysis provides a clue to understand at which scale kinetic and magnetic energies are injected, transferred, and dissipated on the solar surface
- If flows are turbulent at the spatial scale smaller than granules, power-law (scale-free) spectrum is expected up to the diffusion scale.
- It is impossible to spatially resolve the spatial scale where diffusion takes place. But it is important to find how the surface convection makes fine scale magnetic structures, especially at the scale smaller than granulation
  - Are there unresolved "hidden" magnetic flux?
  - Are small-scale magnetic fields created by local dynamo or diffusion of global fields?

Intensity & velocity power spectrum

Frenkiel & Schwarzschild (1955)
Mount Wilson observatory

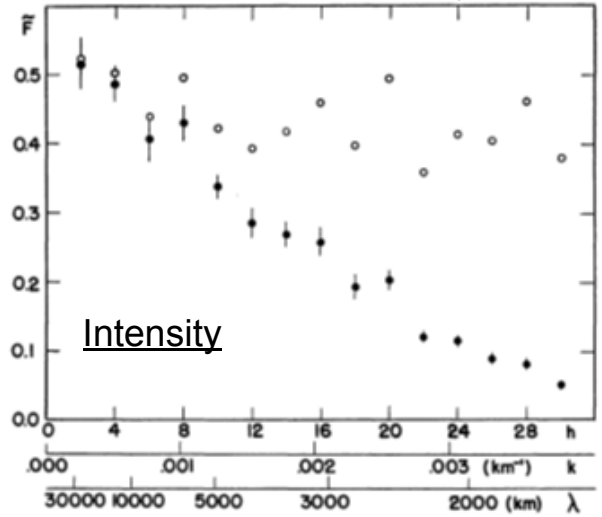

FIG. 2.—Turbulence spectrum in terms of photospheric intensities. The dots show the observed spectrum, with the vertical bars giving the probable errors. The circles show the spectrum corrected for the finite resolution of the plate used.

Muller (1989) MSDP @ Pic du Midi

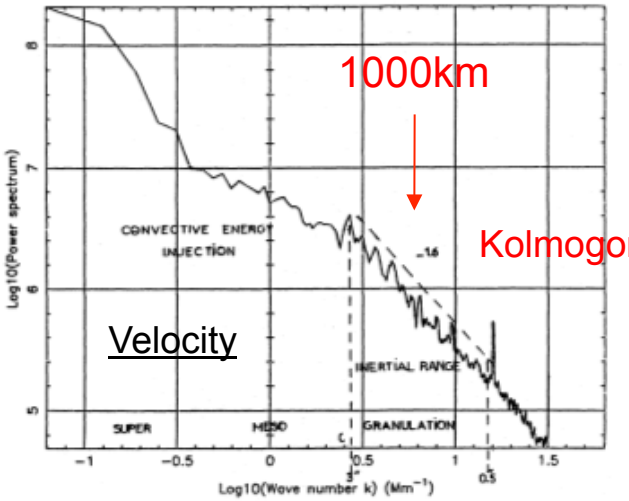

Figure 9. Power spectrum of the solar photospheric motions, derived from two superposed Doppler images taken two and half minutes apart (5 min oscillations filtering).

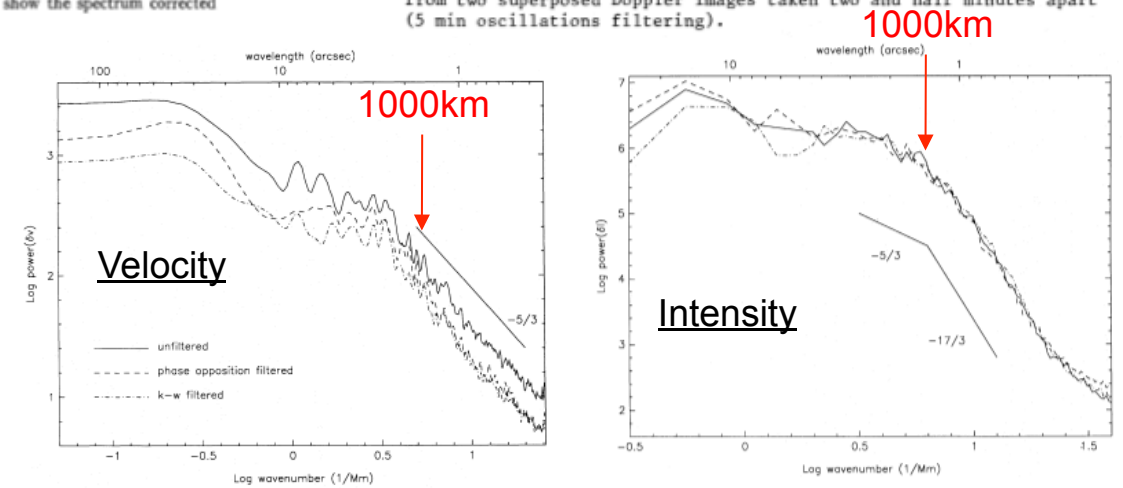

Espagnet et al. (1993)

Magnetic power spectrum

Nakagawa & Priest (1973) Kitt Peak magnetogram

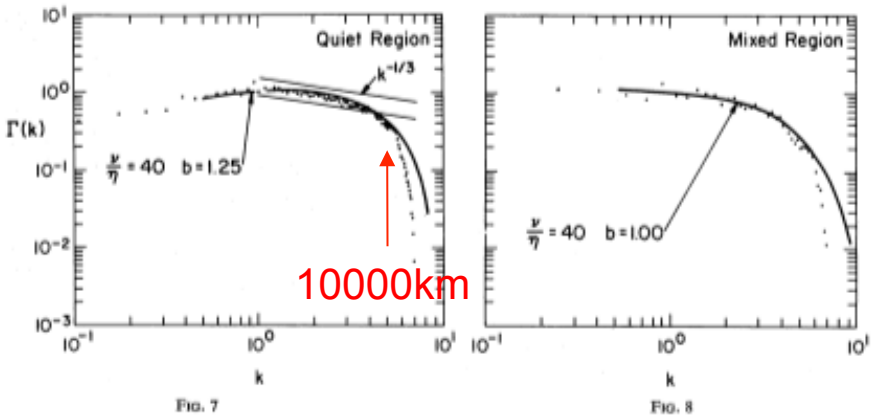

Fig. 7 Fig. 8

Fig. 7.—The comparison of theoretical and observed spectra for a typical quiet region.
Fig. 8.—The comparison of theoretical and observed spectra for a mixed region of activity.

Lee et al. (1997)

Big Bear magnetogram

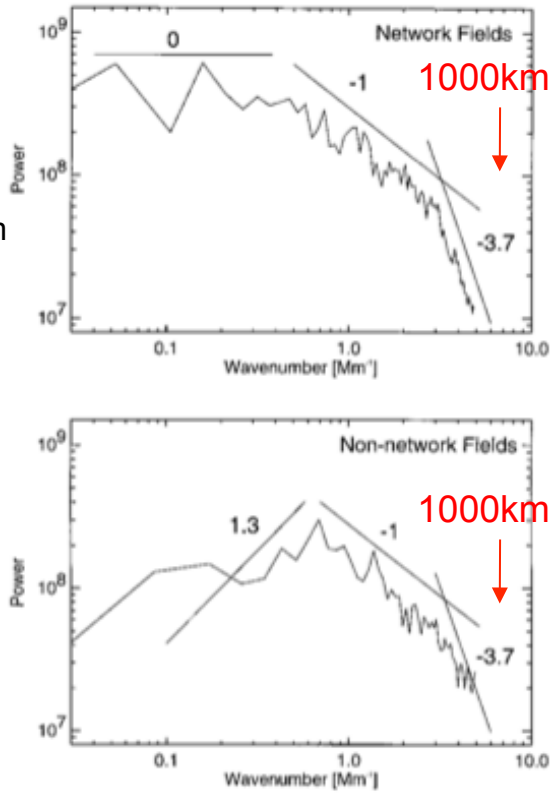

Figure 3. Power spectra of network and non-network fields.

Abramenko et al. (2001)
BBSO and MDI

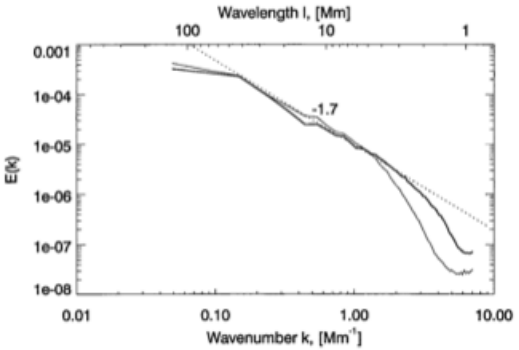

Figure 3. Raw active-region magnetic power spectra obtained from the BBSO (*thin line*) and the MDI (*thick line*) magnetograms. The *dashed line* shows best linear fit $\sim k^{-1.7}$ to both spectra.

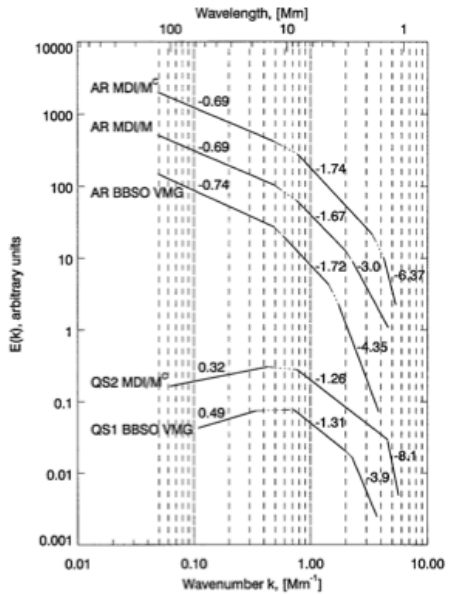

Figure 7. A schematic representation of all the magnetic power spectra obtained in the present study.

Abramenko (2005)
Abramenko & Yurchyshyn (2010)

Studied magnetic power in AR and correlation with flare activitieis

Recent studies using high resolution observations

National Astronomical Observatory of Japan

Rieutord et al. (2010): Hinode SOT NFI and BFI

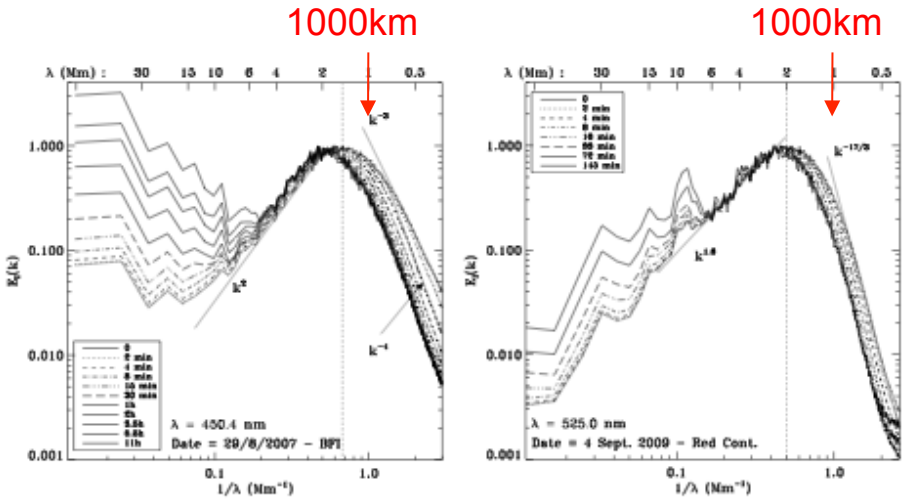

Fig. 9. Spectral energy density of the intensity field. *Left*: data from the BFI at 450.4 nm (spectral width of 0.22 nm sampling the blue continuum) for various time windows (data set of 29-31/8/2007). The spectra are normalised so that the amplitude of the granulation peak is unity. The vertical dotted line marks the position of the granulation peak determined with instantaneous spectra. Here $N_x = 941$, $N_y = 934$ and $N_p = 1024$. *Right*: data from the NFI at 525.0208+0.0108 nm (spectral width of 9 pm sampling the continuum on the red side of the line); here $N_x = N_y = 704$ and $N_p = 1024$.

- Clear peak at the granular scale
- Steeper than the Kolmogorov's -5/3 at the sub-granular scale

Goode et al. (2010), Abramenko et al. (2012): Hinode SOT SP and BBSO

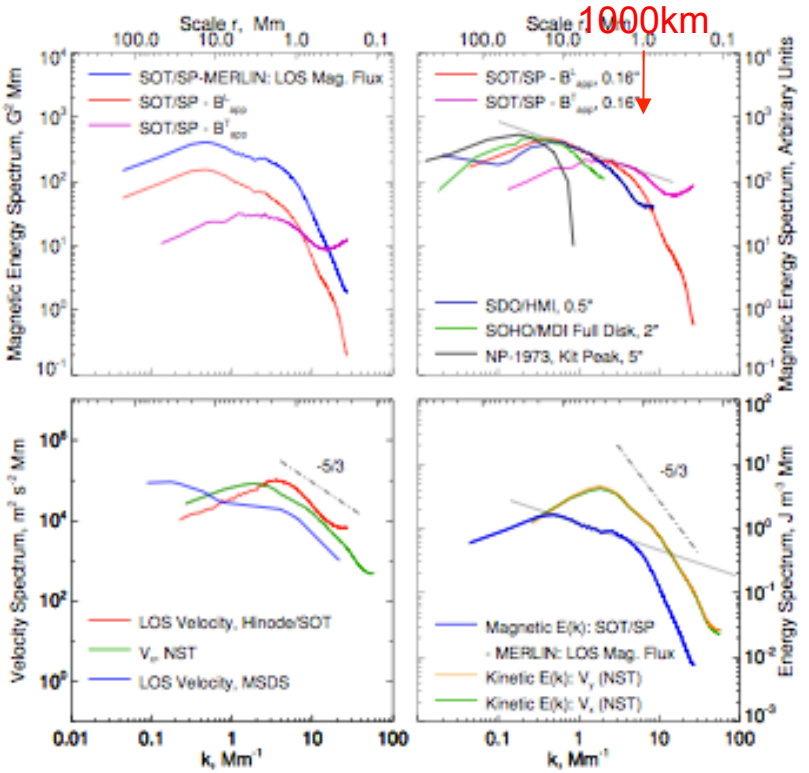

- Horizontal velocities derived with local correlation tracking (LCT).
- It seems the instrument resolution is not corrected to derive the power spectra obtained with Hinode.

HINODE/SOT spectro-polarimetric obs

(Katsukawa & Orozco Suarez 2012)

- Hinode SOT/SP observations to get parameters on the solar surface.
- Because of the stable image quality and accurate polarimetric measurements, the SP data allows us to get the power spectra more accurately.
- We use 30 normal maps (0.15”/pixel) taken at the disk center in 2006 and 2007. Both QS and AR are analyzed .
  QS ($\langle|Bz|\rangle < 20$ G): 23 scans
  QS + AR: 7 scans
- (Bx, By, Bz) are obtained with from wavelength-integrated polarization signals with the method described in Lites et al. (2008)

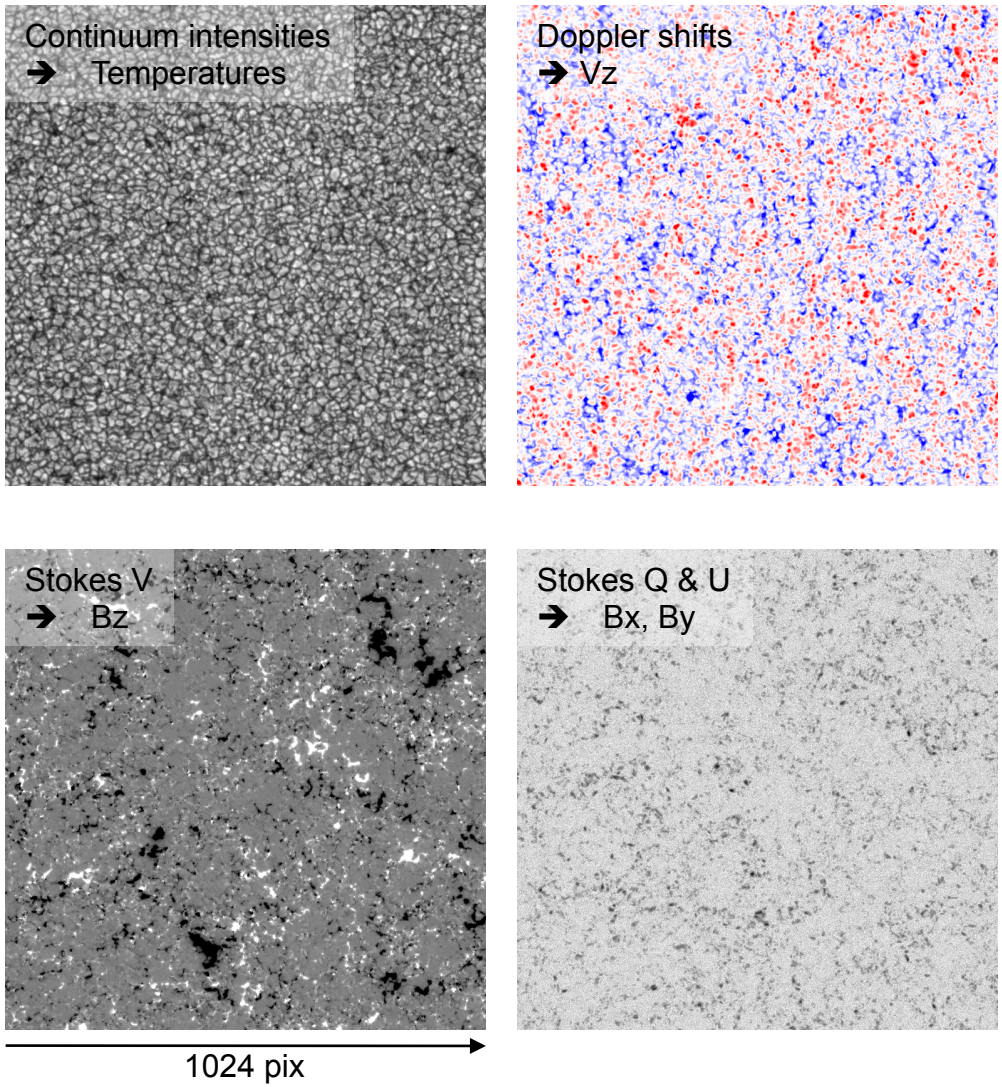

Derivation of the power spectra

- Two dimensional power spectra are derived with 2D-FFT.

$$P(f;k_x,k_y)=\left|\frac{1}{N^2}\sum_x\sum_y f(x,y)\exp\left(-2\pi i(k_x x+k_y y)\right)\right|^2$$

$$f(x,y)=\Delta T \text{ or } v_z \text{ or } B_x \text{ or } B_y \text{ or } B_z$$

- The 2D power spectra are averaged in azimuth of the wave number to get 1D power spectra.

$$P(f;k)=2\pi k\left\langle P(f;k_x,k_y)\right\rangle_{k'\in[k-dk/2,k+dk/2)}$$

- The 1D power spectra are then normalized for each parameters.

Thermal energy

$$E_{th}(k)=\frac{3}{2}\frac{nk_B}{T_0}\frac{P(\Delta T;k)}{dk}$$

Kinetic energy

$$E_{vz}(k)=\frac{1}{2}\rho\frac{P(v_z;k)}{dk}$$

Magnetic energy of horizontal comp.

$$E_{bh}(k)=\frac{1}{8\pi}\frac{\left(P(B_x;k)+P(B_y;k)\right)}{dk}$$

Magnetic energy of vertical comp.

$$E_{bz}(k)=\frac{1}{8\pi}\frac{P(B_z;k)}{dk}$$

Power spectra before the MTF correction

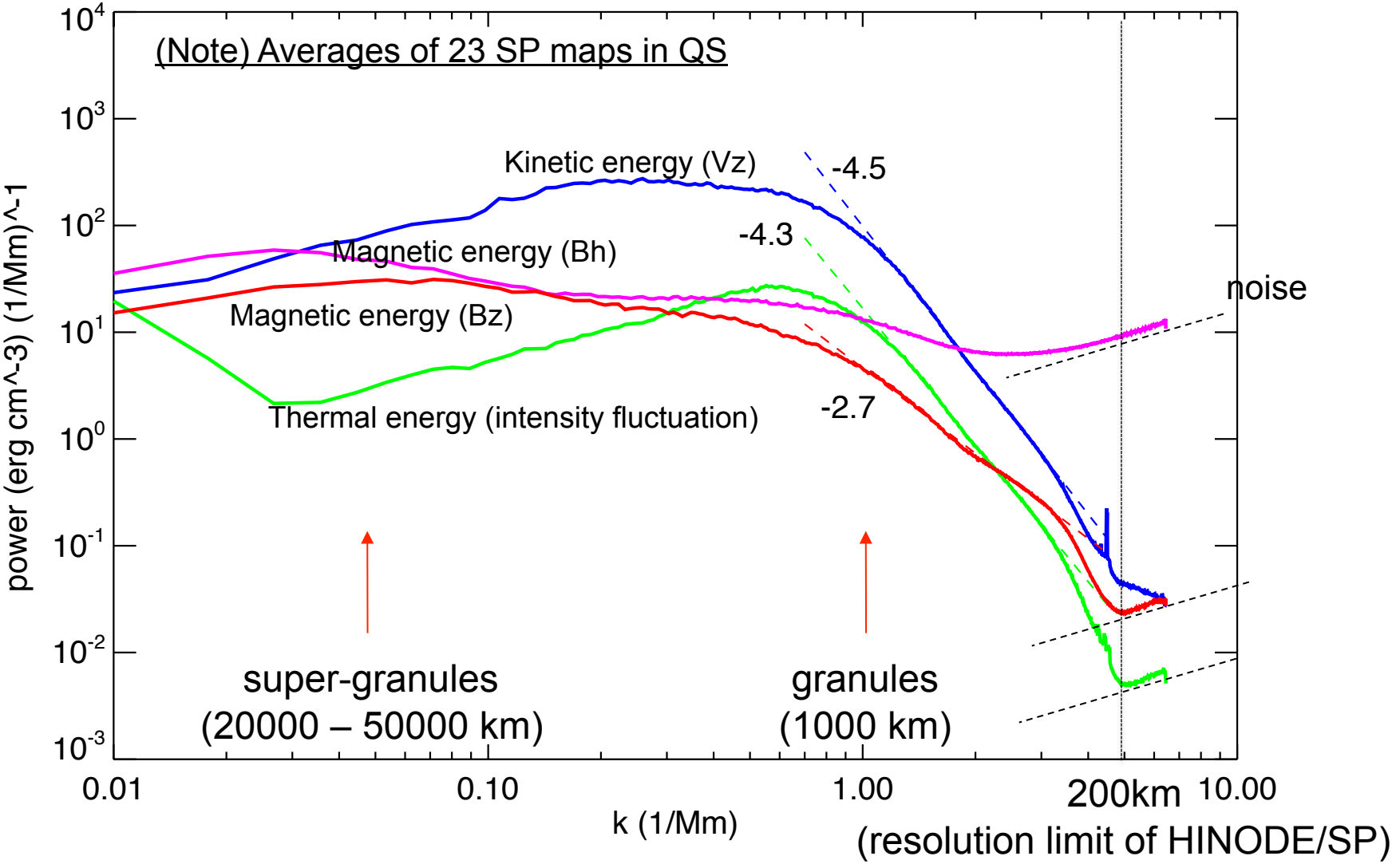

Instrumental MTF and noise correction

- The power spectra thus derived are affected by noises and the instrumental resolution (modulation transfer function, MTF).

$$E'_f(k) = \left(E_f(k) - noise(f,k)\right) \Big/ MTF(k)^2$$

- The noise spectra *noise(f, k)* is estimated using linear fit of the power at high k.

SOT PSF at 630 nm
(Strehl ratio ~0.8)

Provided by Suemtsu

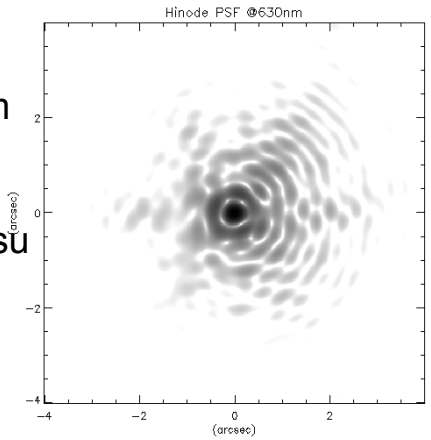

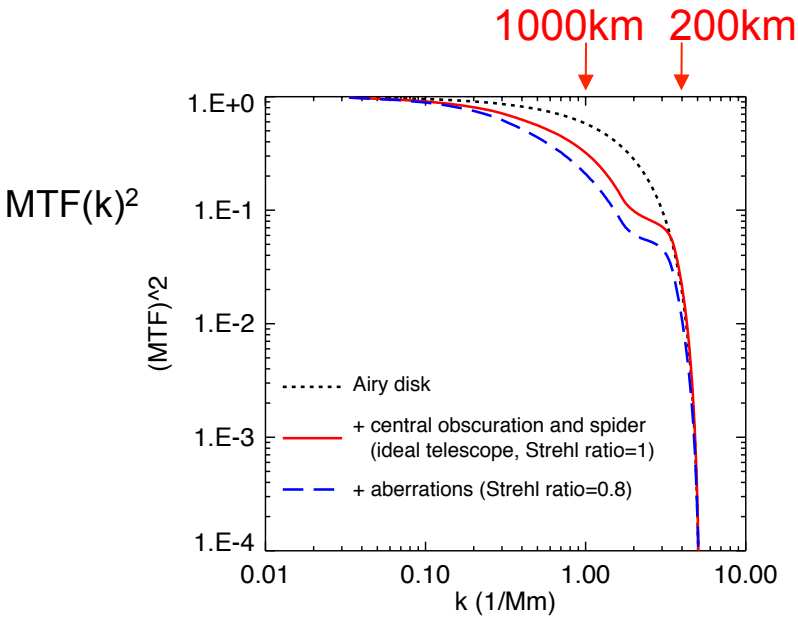

Power spectra after MTF correction

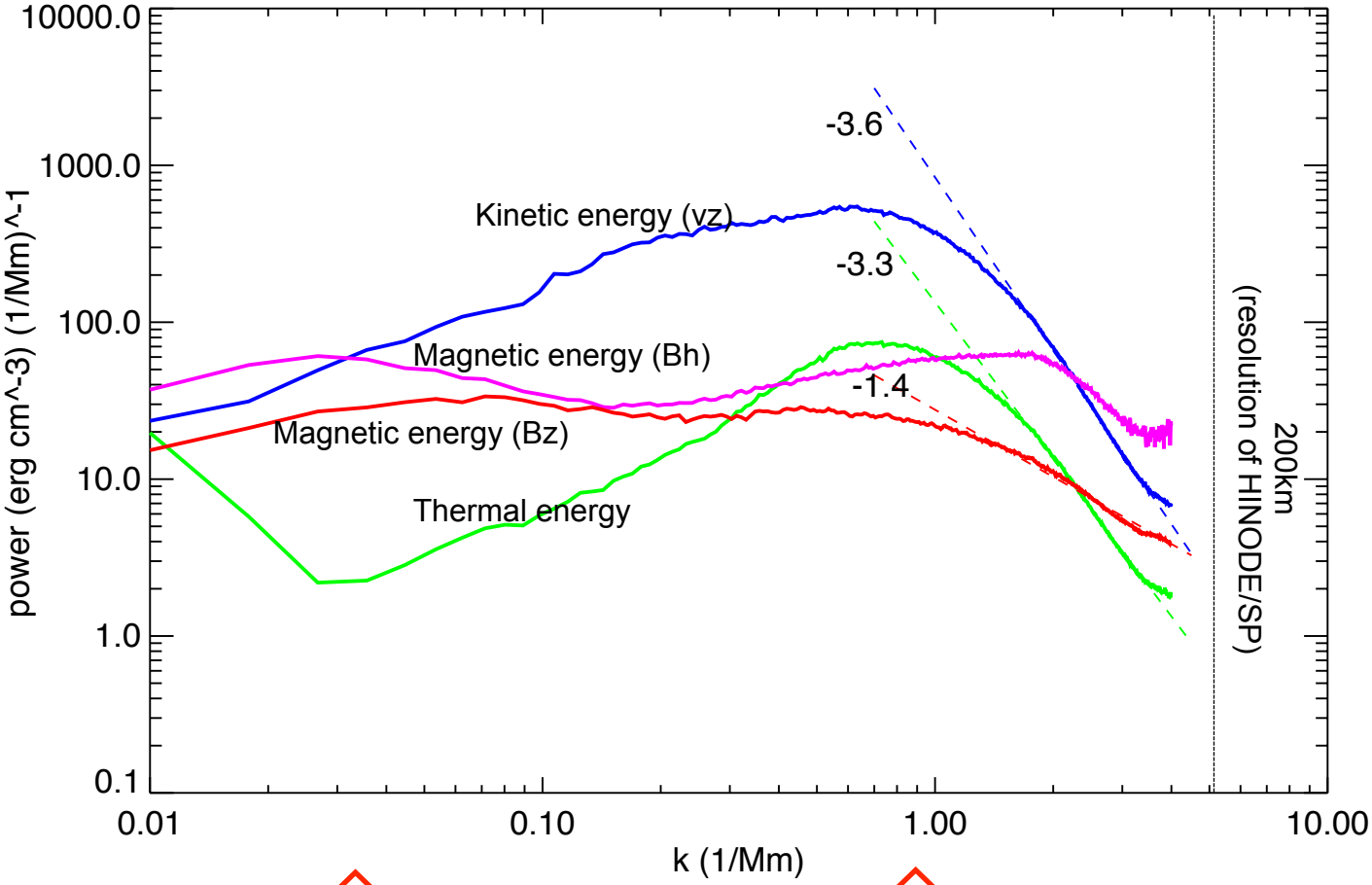

super-granulation
(20000 ~ 50000 km)

granulation
(~ 1000 km)

パワースペクトルの特徴

- The shapes of the intensity & velocity power spectra look very similar. It is expected because of good correlation between the intensities and the Doppler velocities at the granular scale.

- Both the spectra have clear peak at the granular scale (~1000 km). No enhancements at the super-granular and meso-granular scales.

Velocity-intensity correlation (Hinode-SP)

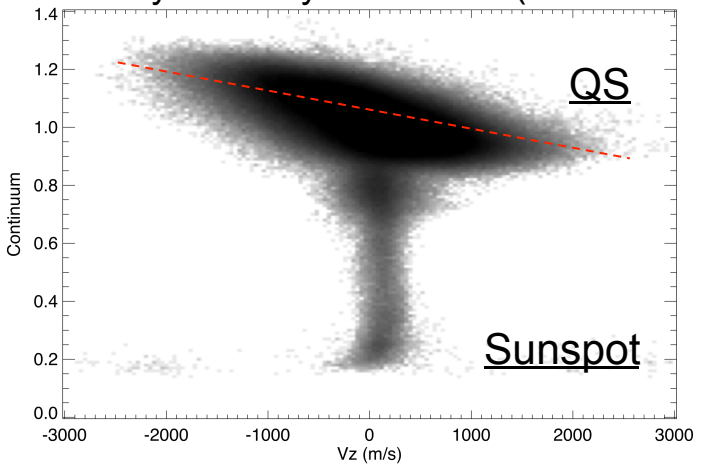

- The power-law indices of the slopes are -3.6 ~ -3.3, which are significantly steeper than the Kolmogorov's -5/3 law.

- Both the horizontal and vertical powers distribute over a broad wavenumber range. Weak enhancements at the granular and super-granular scales, which suggests that the these are typical scales characterizing the magnetic field distribution on the solar surface. No enhancements at the meso-granular scale.

Power spectra in small boxes

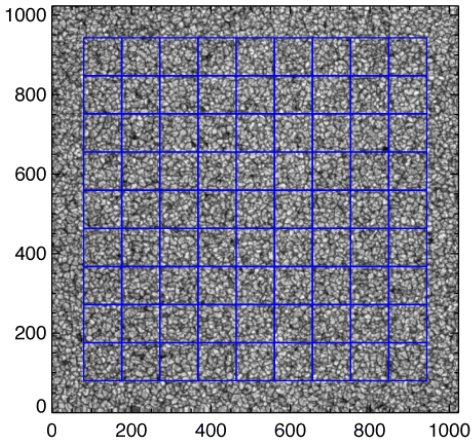

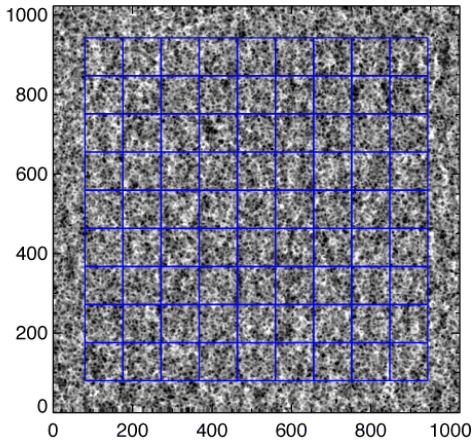

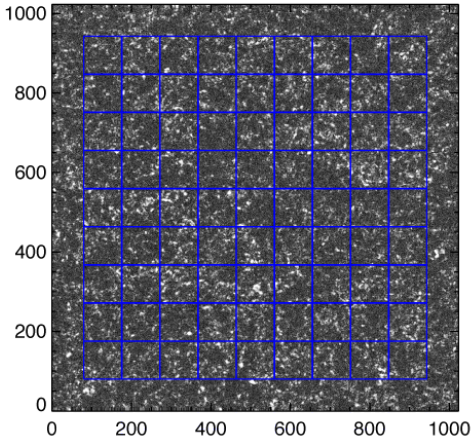

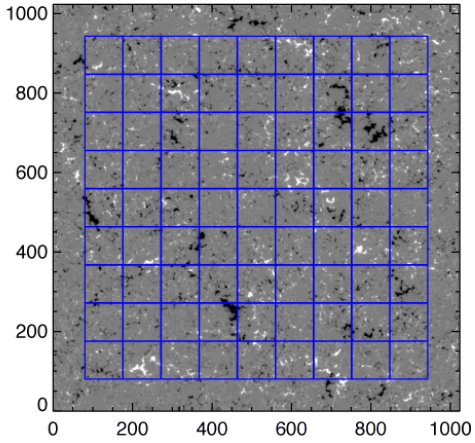

- To separate internetwork and network structures, the 1024x1024 FOV is divided into small boxes whose FOV is 96x96 (~10^4 kmx10^4km). The FOV is not enough to cover the super-granular scale.
- MTF+noise corrections are applied.
- We derive average unsigned flux density <|Bz|> in each box. The power spectra are averaged over each <|Bz|> interval.
- Compare the power spectra with <|Bz|>.

Power spectra in internetwork regions

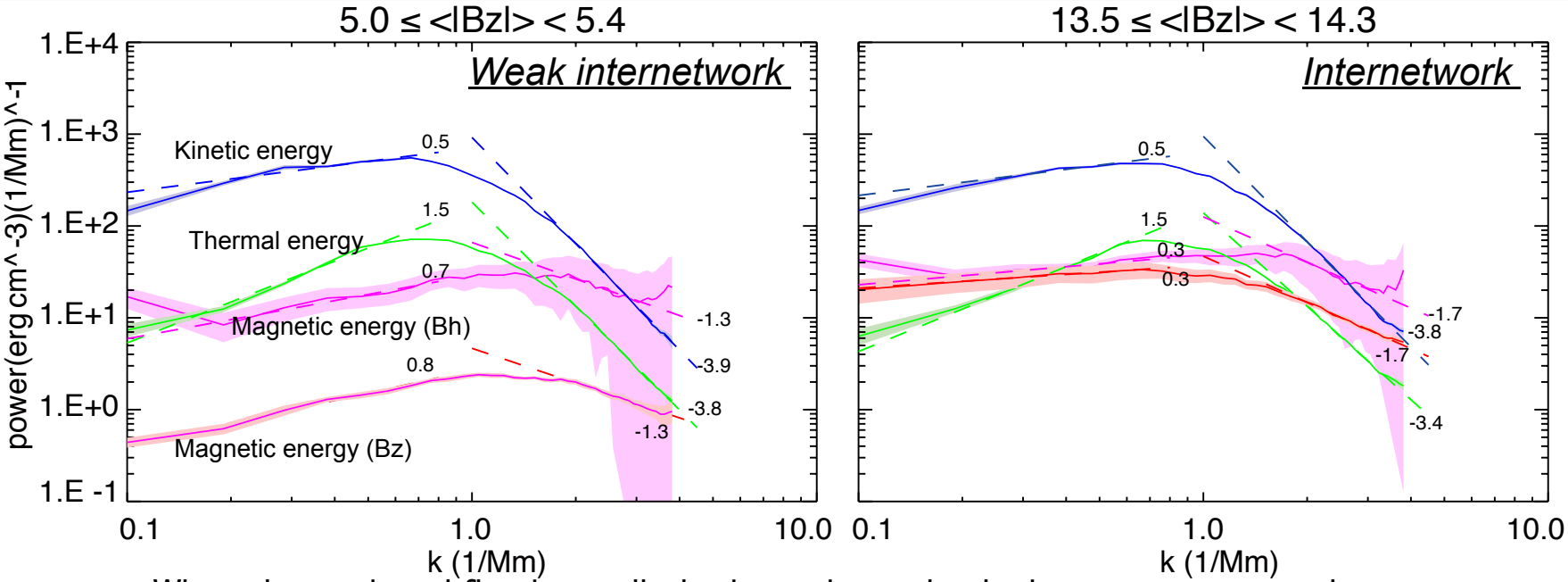

- When the unsigned flux is small, the intensity and velocity power spectra do not change much. Peaks at the granular scale. The power law indices are steeper than −3 at the sub-granular scale.
- The horizontal and vertical magnetic power spectra have similar shapes, and both the spectra have peaks at ~800 km. Consistent with the size of the granular scale horizontal field structures (Ishikawa & Tsuneta 2010, Orozco Suarez & Katsukawa 2012).
- Horizontal magnetic power is larger than the vertical one (Lites et al. 2008).

Probability density function (PDF) in QS

Orozco Suarez & Katsukawa (2012)

- The shape of the inclination distribution for weak fields results from the presence of loop-like magnetic and not from tangled fields within the field of view.

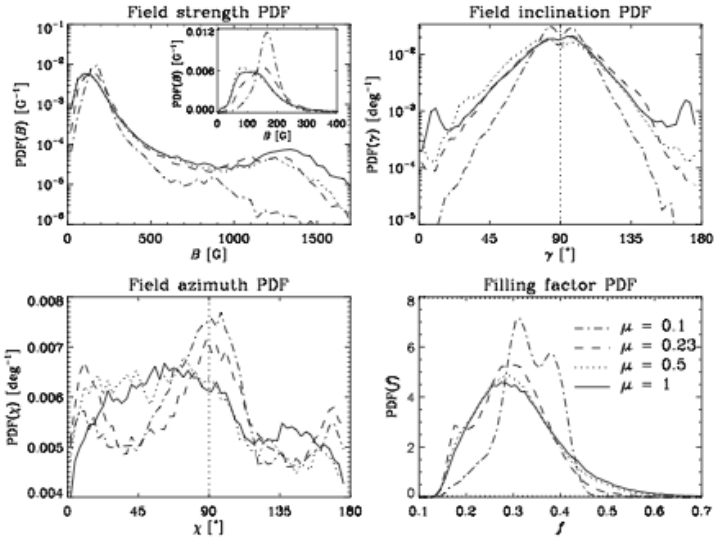

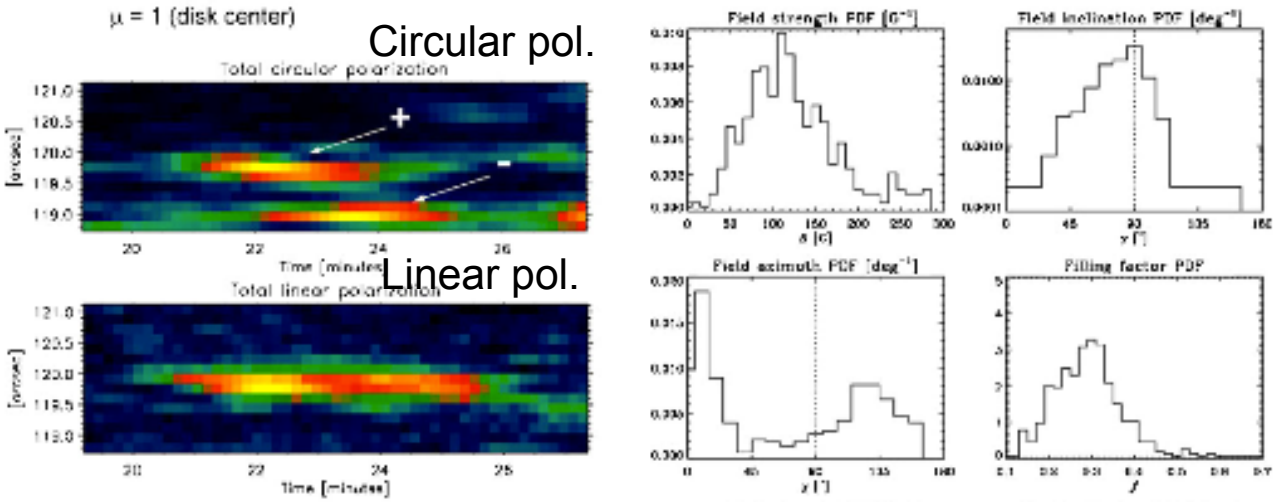

Power spectra in network and AR

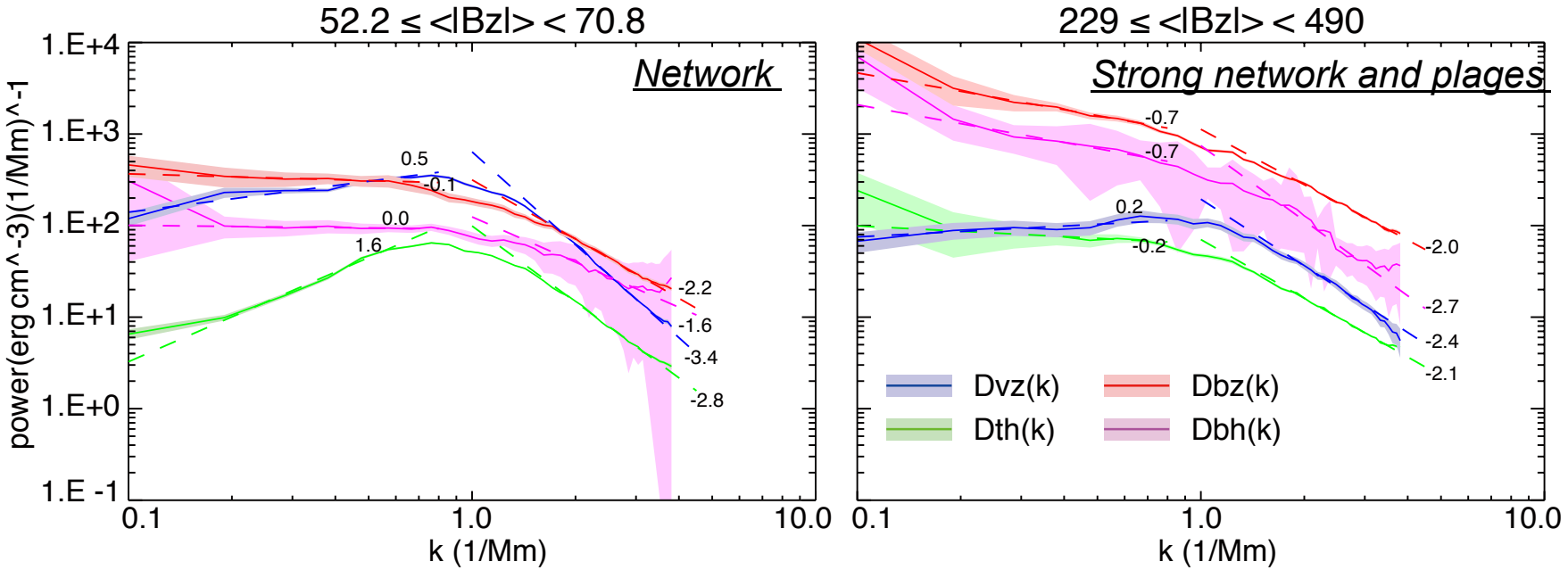

- The magnetic power tend to increase especially in the lower wavenumber range. The slopes changes their signs from positive to negative, which makes the peak at the granular scale less pronounced in the network regions.
- The slopes of the velocity and intensity power spectra become less steep at the sub-granular scale.
  - Suppression of the power at the granular scale (suppression of granular convection)
  - Enhancements of the power in the high wavenumber range (contribution of facular structures)
- All the power spectra exhibit similar slopes at the sub-granular scale when the average unsigned flux is larger than 100 G.

Power indices vs <|Bz|>

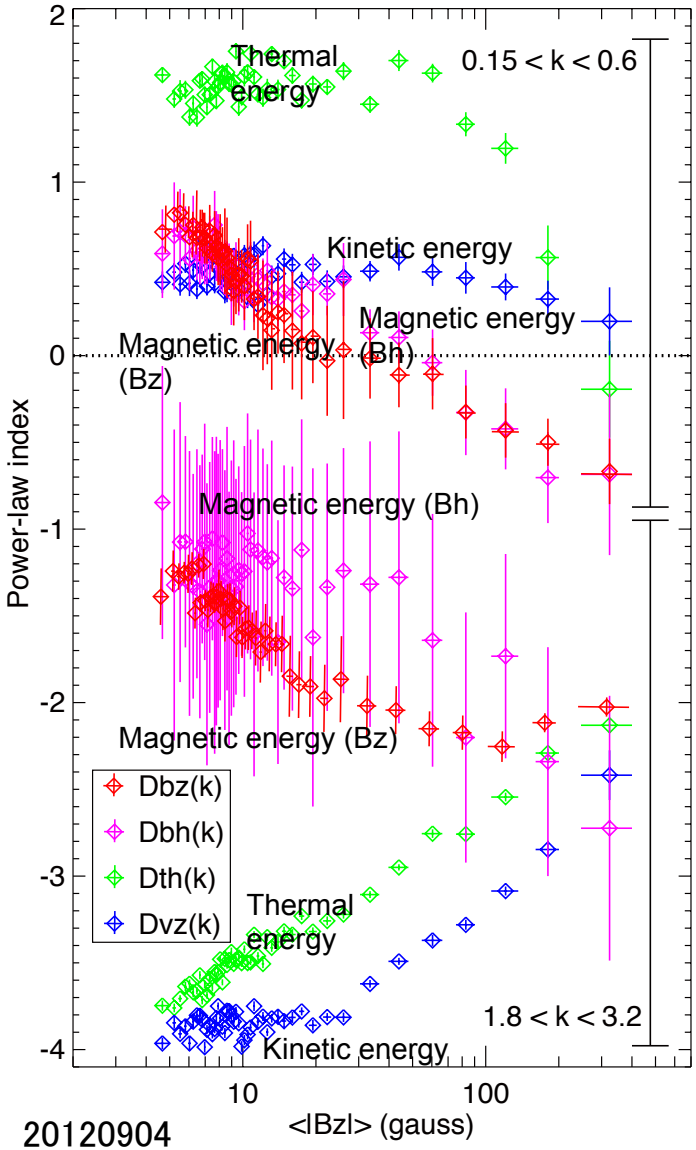

k <1 Mm^{-1} (Larger than the granular scale)

k>1 Mm^{-1} (Smaller than the granular scale)

- The slope at high k (sub-granular scale) tends to become positive (= less steep) for thermal and velocity power spectra.
- The slope at high k (sub-granular scale) tends to become negative for Ebz when <|Bz|> <100.
- The power law slope becomes almost identical (~ −2) among all the power spectra when <|Bz|> > 100.
- The slope at small k tends to become negative. The peak at the granular scale disappears when the unsigned flux becomes large.

Power indices vs <|Bz|>

- When the magnetic energy is smaller than the convective energy (B<100G), the power spectra of intensities and velocities are completely different from those of Ebz and Ebh. The difference of the power-law indices are about 2.

  ➔ In this regime, magnetic fields are passively advected by convective motion. One possibility is that $(\nabla \cdot V)$ or $(\nabla \times V)$ create magnetic structures, which creates $Eb(k) \propto k^2 Ev(k)$.

- When the magnetic energy becomes large (B>100G), the shapes of the power spectra (power-law indices) become similar at the sub-granular scale. Strong interaction between convection and magnetic fields takes place at every spatial scales.

What is the predominant magnetic structure

- The total magnetic energy is:

$$E_B(k) \propto k^{\alpha}$$

$$E_B \propto \int_{k0}^{k1} k^{\alpha} dk = \frac{1}{1+\alpha}\left[k^{1+\alpha}\right]_{k0}^{k1}$$

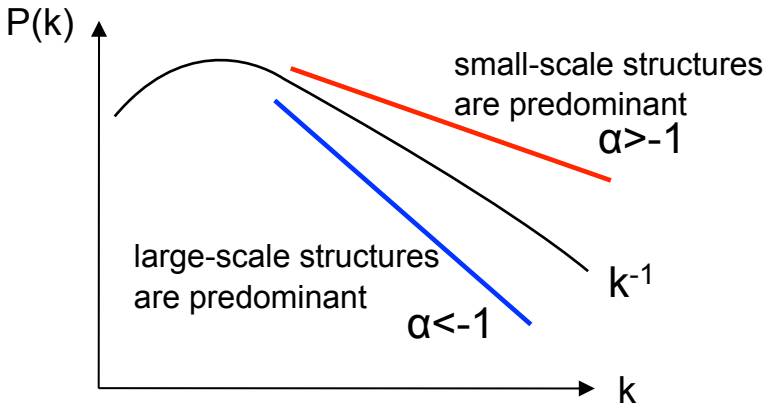

- In the observations with Hinode SP, $\alpha \approx -1$ or $\alpha < -1$.

  This means that the total magnetic energy mainly comes from either the granular-scale magnetic structures or both the granular-scale and smaller ones contributing evenly.

What is the predominant magnetic structure

- If we extrapolate the power spectrum of $k^{-1.3}$ up to 50/Mm, the percentage of the magnetic energy contained in the observed wavenumber range is ~50 %.
- Numerical simulations reproducing local dynamo suggested that small-scale structures are important, and more magnetic energies at the unresolved scale.

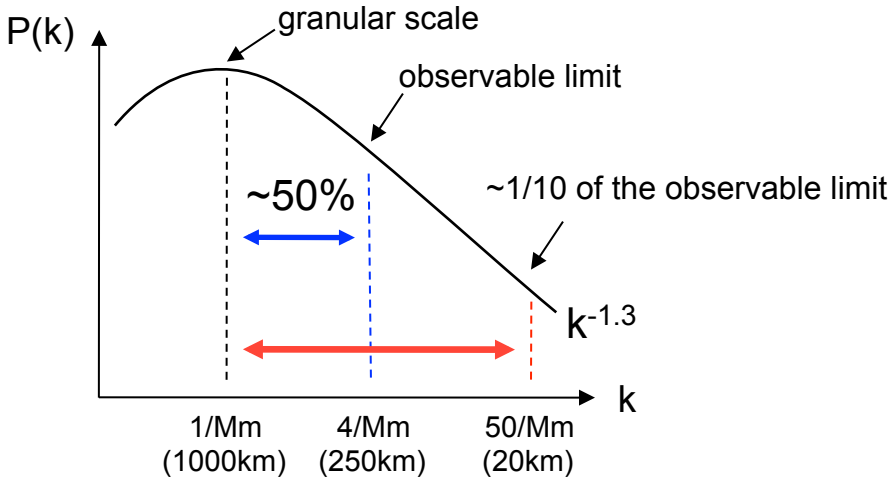

Vogler and Schussler (2007) Pietarila Graham et al. (2009, 2010)

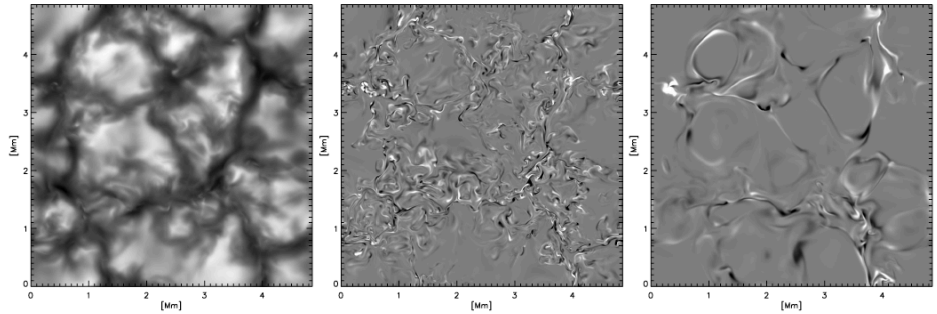

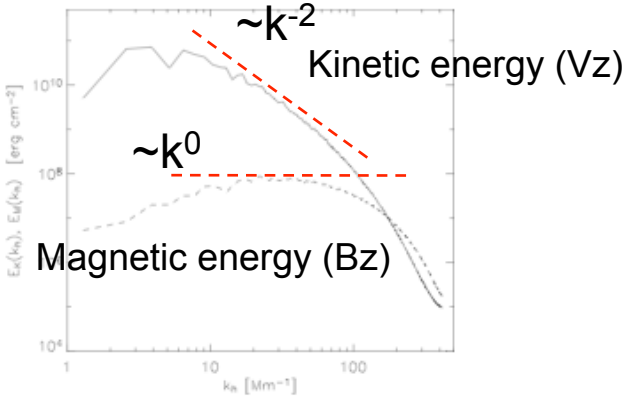

ALMAでまずやるべきこと

- ALMAで得られる新しい情報
  - 0.1” (70 km) より小さい構造のフーリエ成分を取得
  - 粒状斑スケール (~1000km)から<100kmスケールにかけての温度構造を(離散的な)パワースペクトルとして求める
  - 必ずしも増合成は必要ない
- そのためには
  - なるべく高周波数 (基線長2kmの場合)
    - 0.126” @ 300 GHz (Band7)
    - 0.054” @ 700 GHz (Band9)
    - 0.040” @ 900 GHz (Band10)

    (Band9 – Band10で見えるのは温度最低層のあたり)
  - 視野: 5”程度でも十分 (粒状斑が数個分入る大きさ)
  - 時間分解能: <1 min (できたら<10sec)

- ターゲット
  - 太陽面内の複数の静穏領域で上記を取得し、その領域の平均磁束密度との関係を調べる
  - Internetwork (磁場が弱い場所, $\langle|Bz|\rangle < 10$ Mx cm^{-2})
  - Network (磁場が比較的強い場所, $10 < \langle|Bz|\rangle < 50$ Mx cm^{-2})

フラックスチューブ成分

- 対流によって作られる磁場構造とともに、collapseしたフラックスチューブの成分がエネルギー的には重要ではないか？（Stenflo 2012）
- 空間スケール10–100 km ~ photon mean free path
- フラックスチューブ成分により、パワースペクトルに折れ曲がりが見える

- 本当か? どの程度のエネルギーの寄与か?

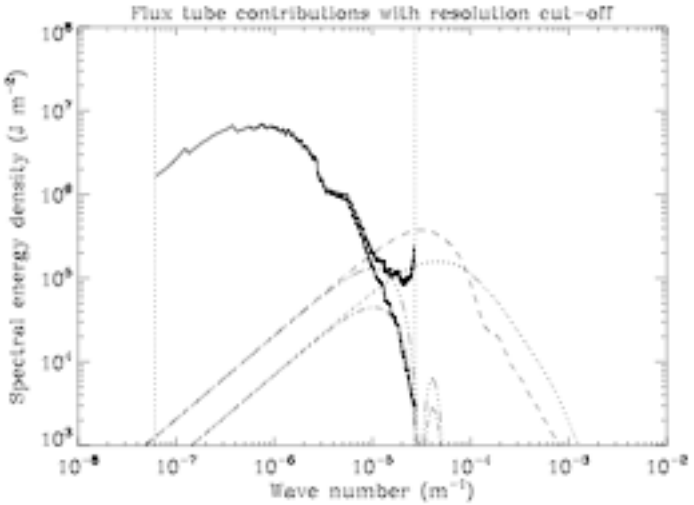

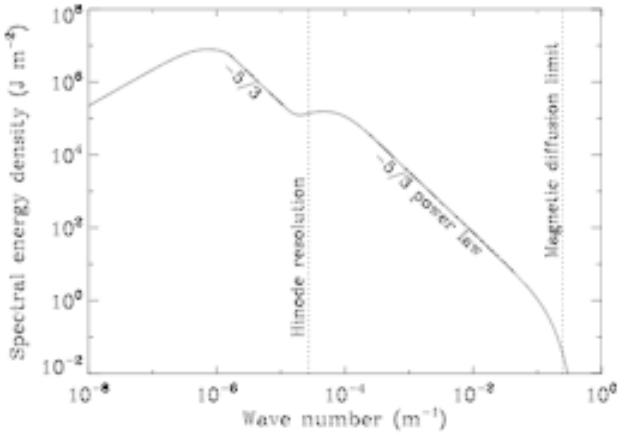

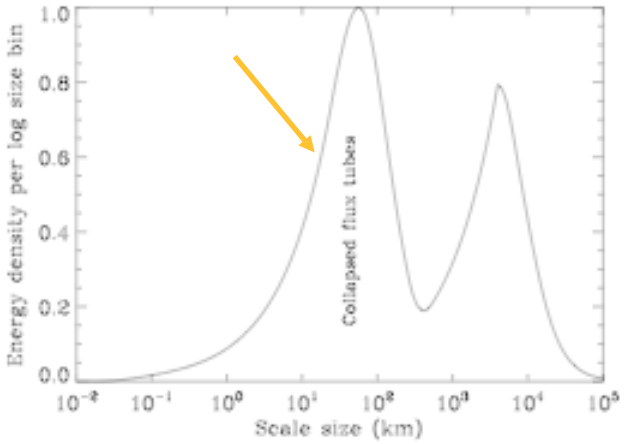

光球−彩層にかけての対流・磁場構造

- 光球でも上層と下層での違いを見るため、ひので−SPでbisector解析を実施。
- Line coreのintensity → ~4800 K (高さ~300km)

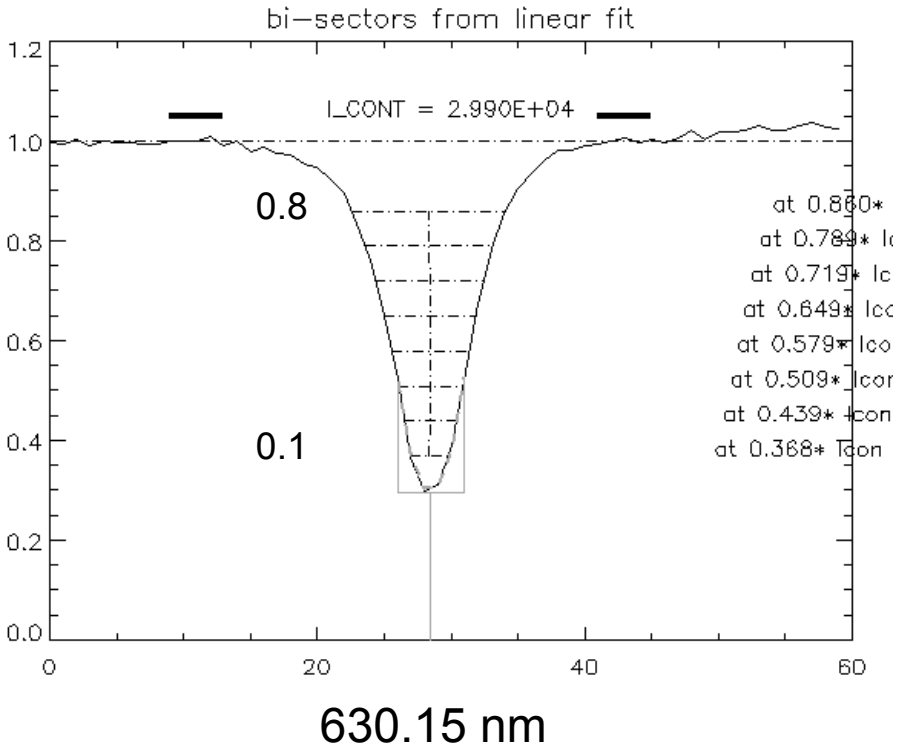

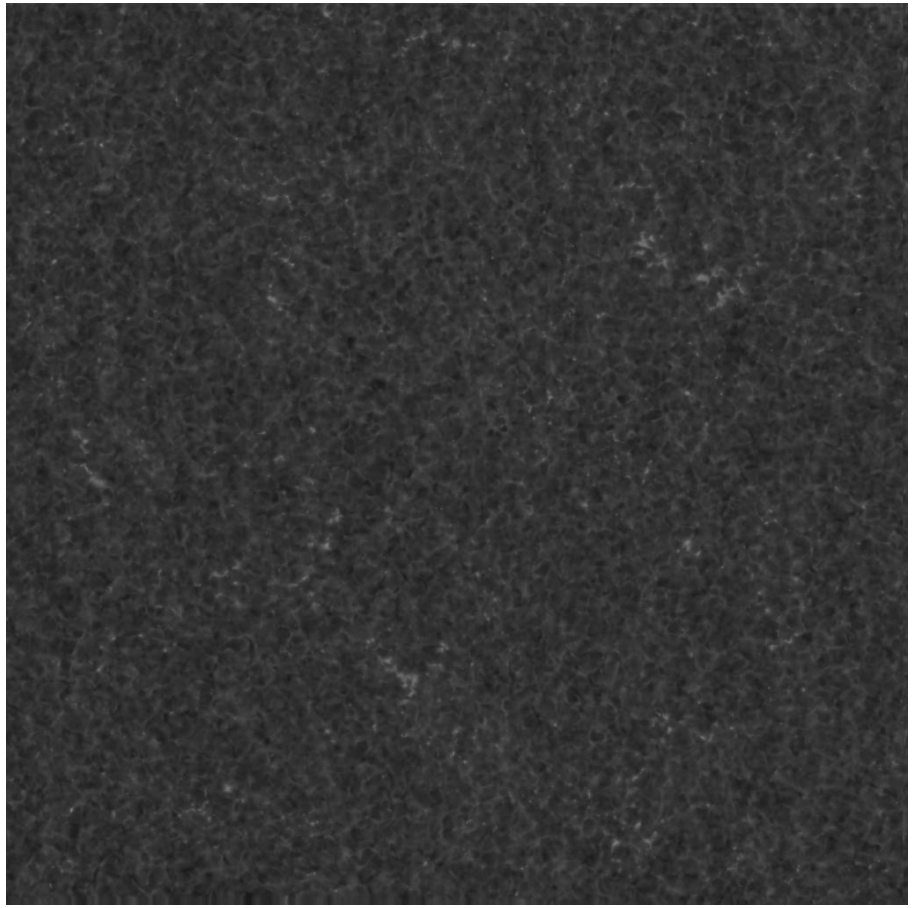

Temperature

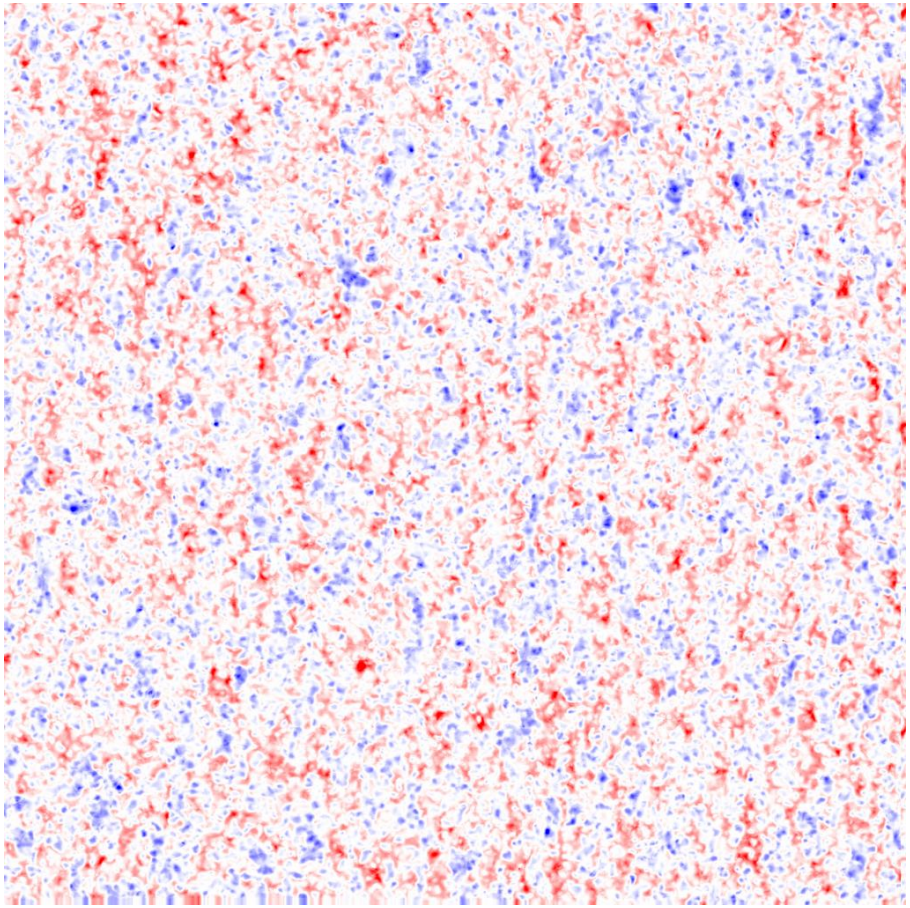

Velocity

光球上部のパワースペクトル

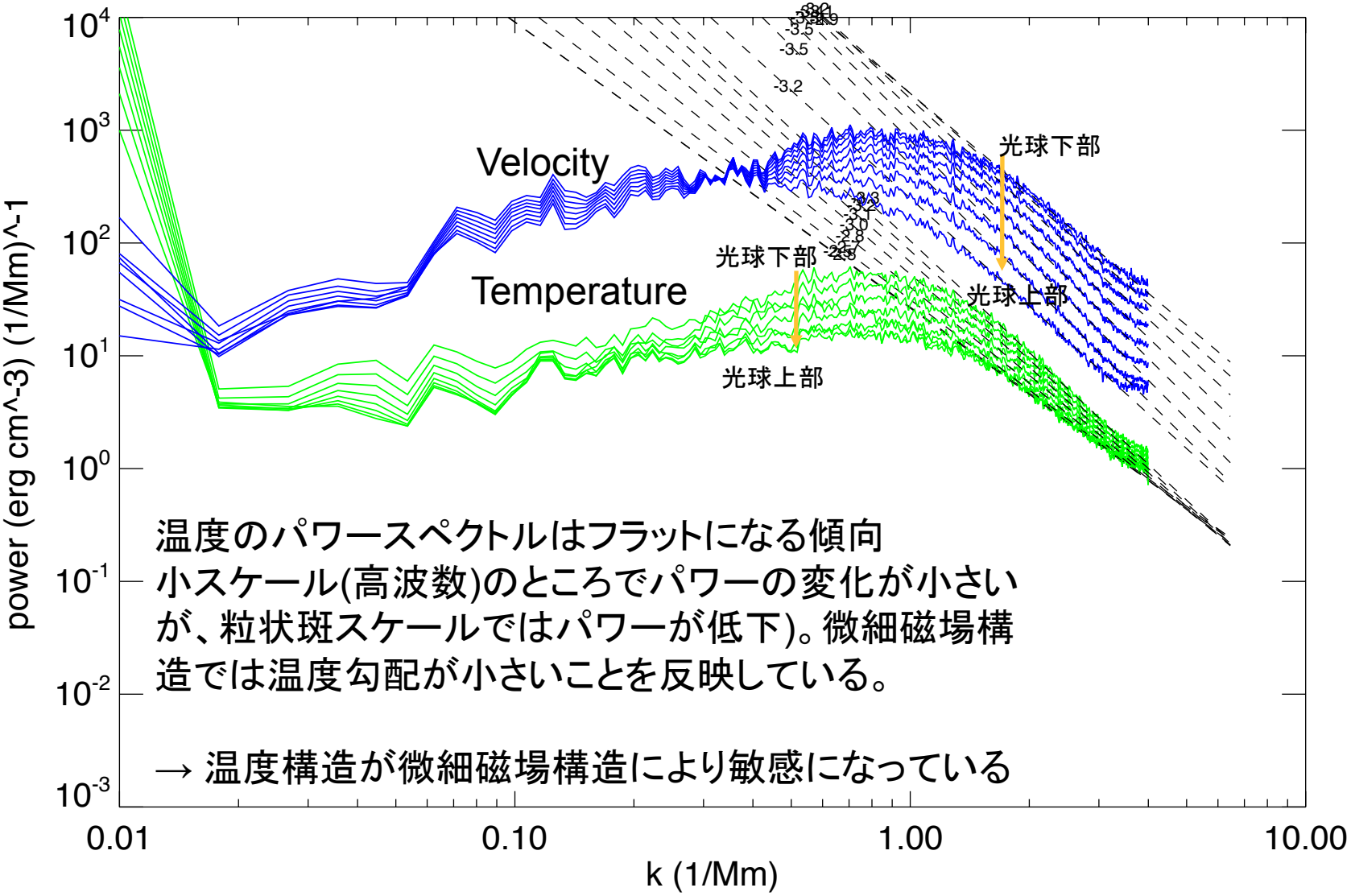

HINODE/SOT FG

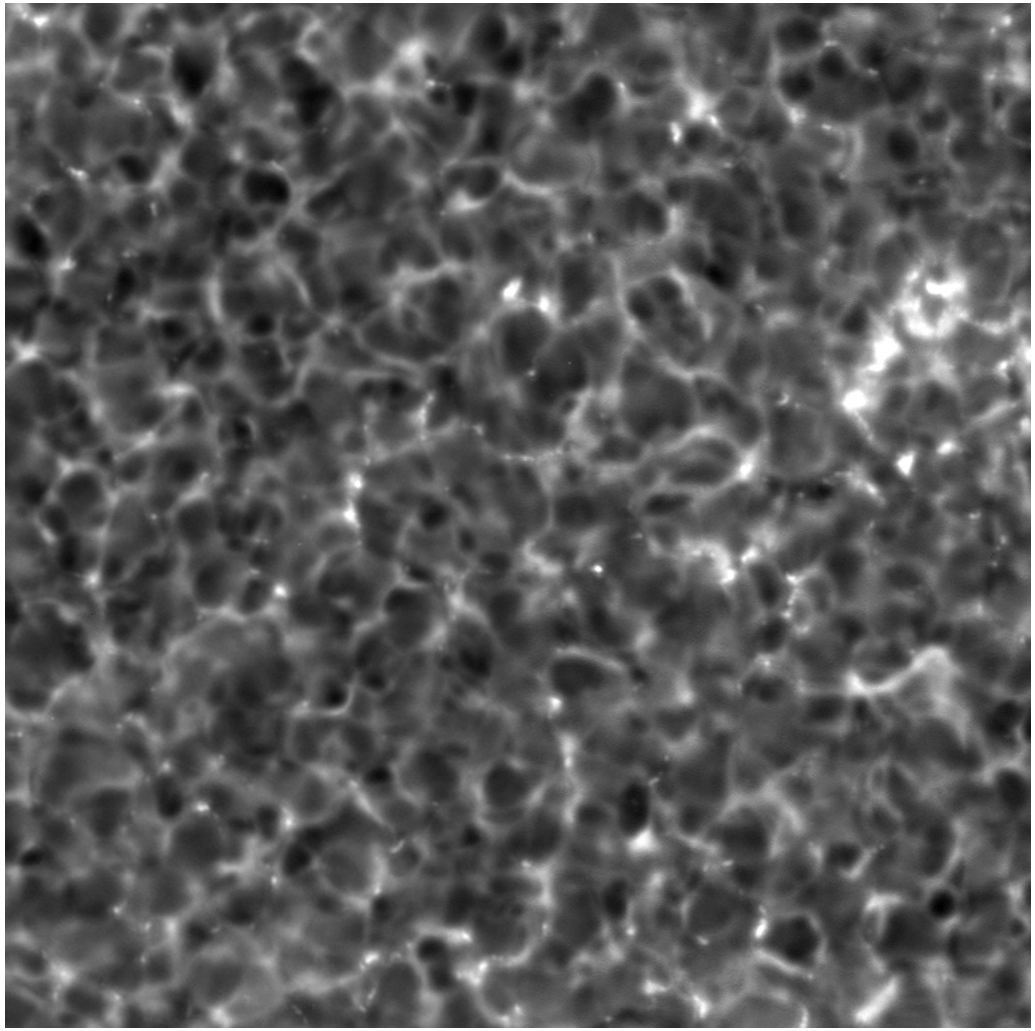

Continuum

G-band

Ca II H

Power spectra obtained from the FG obs

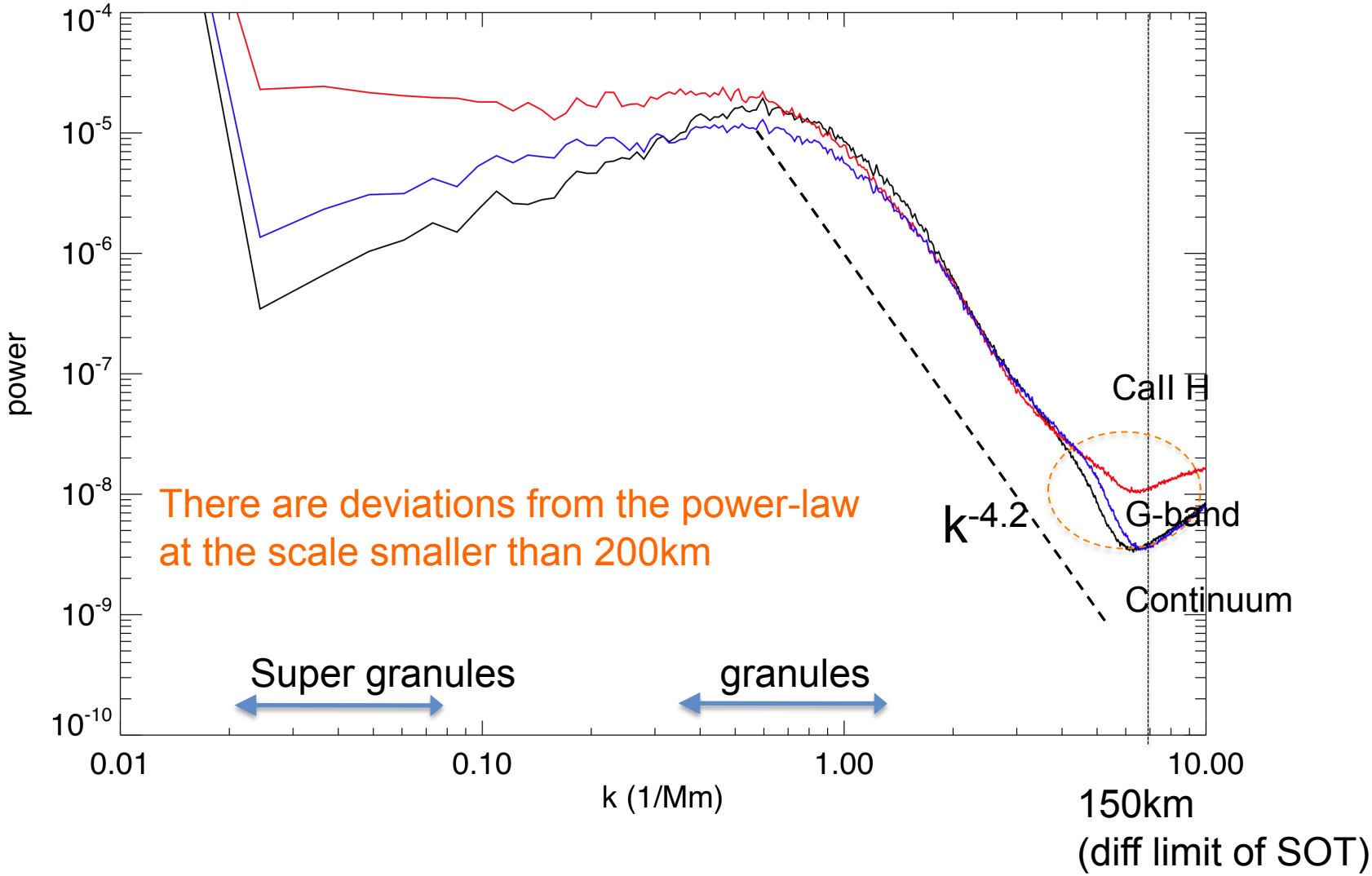

まとめ

- 近年、ひので や地上望遠鏡による高解像度観測の進展によって、粒状斑スケール、あるいはそれよりも小さなスケールでの対流の振る舞い、それによる磁場構造の形成が調べられるようになってきている
  - Power spectra steeper than the Kolmogorov's −5/3 power-law
  - Total flux budget (hidden magnetic flux?)
  - Local dynamo
  - Convective collapse

- ALMAによる観測から
  - 温度最低層のあたりの温度の微細構造の決定
  - ~100kmのフラックスチューブ成分はあるのか? それとも粒状斑スケールから連続的か
  - 大スケール(粒状斑)構造と小スケール構造のどちらがエネルギー的に重要か